PHYSICAL REVIEW LETTERS

How White Noise Generates Power-Law Switching in Bacterial Flagellar Motors

Yuhai Tu and G. Grinstein

IBM Research Division, T. J. Watson Research Center, P.O. Box 218, Yorktown Heights, New York 10598, USA

The clockwise (CW) or counterclockwise (CCW) spinning of a bacterial flagellar motor is controlled by the concentration $[Y]$ of a phosphorylated protein, CheY-P. Representing the stochastic switching behavior of the motor by a dynamical two-state (CW and CCW) model, whose energy levels fluctuate in time (t) as $[Y](t)$ fluctuates, we show that temporal fluctuations in $[Y](t)$ can generate a power-law distribution for the durations of the CCW states, in agreement with recent experiments. Correlations between the duration times of nearby CCW (CW) intervals are predicted by our model, and shown to exist in the experimental data and to affect the power spectrum for motor switching.

Introduction.—Bacterial chemotaxis is one of the most fascinating sensory systems in biology. Most of the relevant proteins in the underlying biochemical network have been identified, and their interactions elucidated, making it one of the most suitable biological systems for quantitative systems-level analysis similar to that commonly performed on physical systems. The bacterial chemotaxis machinery has two parts: the signaling pathway and the flagellar motor (for recent reviews, see [1–3]). The motor has two possible states of motion, spinning either clockwise (CW) or counterclockwise (CCW). In *E. Coli*, for example, each cell has roughly 4–6 flagellar motors distributed randomly around its rod-shaped body. When all the motors rotate CCW, the flagella form a coherent bundle and the cell "runs," i.e., moves in a straight line; when one or more of the motors rotate CW, the flagellar bundle disassembles and the cell "tumbles," i.e., rotates randomly without moving. The signaling pathway controls the switching of the motor between the two states by regulating the phosphorylated form of a signaling molecule, CheY-P, higher concentration of CheY-P leading to higher probability of CW rotation.

Recently, single-cell experiments were performed on wild type (WT) *E. Coli* cells, with long measurements (up to 170 min) of the motor's switching behavior [4]. Surprisingly, the distribution of CCW duration times exhibited a power-law tail, not the Poisson-like distribution of conventional expectation [5]. Although such non-Poisson behavior was observed previously in minicells [6], Ref. [4] was the first to identify the power-law distribution and study the corresponding time series of the binary switching pattern, whose power spectrum at low frequency appears to exhibit $1/f$-type behavior.

What causes the power-law CCW duration distribution? How does this distribution affect the power spectrum of the switching time series? In this Letter, we propose and analyze a dynamical two-state model for the motor switching dynamics to address these questions.

Model and duration distributions.—Following Khan and Macnab [7], we treat the bacterial motor system as a two-state model with each state (CW or CCW) sitting in a potential well, transitions between the states governed by thermal fluctuations over an energy barrier. Let the free energy barriers for CCW to CW and CW to CCW transitions be ΔG_0 and ΔG_1, respectively. Then the switching rates between the CCW and CW states are $k^+ = \omega_0 \times \exp(-\Delta G_0/k_B T)$ and $k^- = \omega_0 \exp(-\Delta G_1/k_B T)$, with ω_0 the attempt frequency and $k_B T$ the thermal energy. As illustrated in Fig. 1, the energy barriers $\Delta G_{0,1} = \Delta G_{0,1}([Y](t))$ vary in time due to their dependence on the CheY-P concentration, $[Y](t)$, which fluctuates due to the intrinsic stochastic nature of the signaling pathway kinetics and the relatively small number of protein molecules in the cell.

In a constant external environment, $[Y](t)$ can be written as $[Y](t) = [Y]_0 + \delta[Y](t)$, with $[Y]_0$ the (constant) mean value. The fluctuation $\delta[Y](t)$ can be well characterized by its standard deviation $\Delta[Y]$ and its correlation time τ.
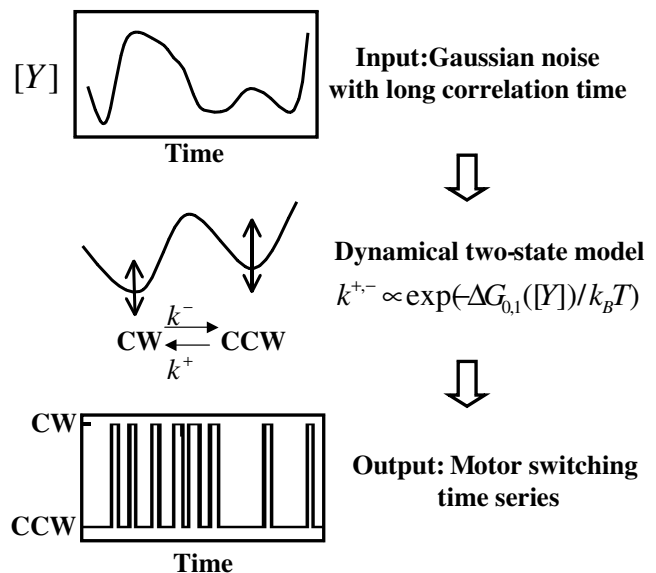

FIG. 1. Illustration of the dynamical two-state model. $[Y]$ is the time dependent CheY-P concentration.

When $\delta[Y](t)$ is much smaller than the mean, i.e., $\delta[Y] \ll [Y]_0$, the energy barriers can be approximated by linear expansion:

$$\frac{\Delta G_{0,1}([Y])}{k_B T} \simeq \frac{\Delta G_{0,1}([Y]_0)}{k_B T} + \alpha_{0,1} \frac{\delta[Y]}{[Y]_0}, \quad (1)$$

where $\alpha_{0,1} = \frac{\partial \Delta G_{0,1}}{k_B T \partial \ln[Y]}|_{[Y]=[Y]_0}$ are two dimensionless constants characterizing the steepness of the response curves of the motor, both of them depending on $[Y]_0$ and parameters for the bacterial motor.

The CheY-P correlation time τ, dominated by slow methylation kinetics [3], should far exceed the characteristic switching times t_0 and t_1 defined by $t_{0,1} = \omega_0^{-1} \exp(\Delta G_{0,1}([Y]_0)/k_B T)$, i.e., $\tau \gg t_{0,1}$. Therefore, the fluctuating piece, $\delta[Y](t)$, of the CheY-P concentration is approximately constant during each individual CCW or CW interval, whose time duration $\tau_{0,1}$ is drawn from the Poisson distribution, $P(\tau_{0,1}, \tilde{\tau}_{0,1}) = \frac{1}{\tilde{\tau}_{0,1}} \exp(-\frac{\tau_{0,1}}{\tilde{\tau}_{0,1}})$, with characteristic times $\tilde{\tau}_{0,1}$ given by $\tilde{\tau}_{0,1} = t_{0,1} \exp(\alpha_{0,1}\delta[Y]/[Y]_0)$. From the distribution $P(\delta[Y])$ of $\delta[Y]$, and the exponential dependence of $\tilde{\tau}_{0,1}$ on $\delta[Y]$, one easily obtains the distributions $\tilde{Q}_0(\tilde{\tau}_0)$ and $\tilde{Q}_1(\tilde{\tau}_1)$, for $\tilde{\tau}_0$ and $\tilde{\tau}_1$:

$$\tilde{Q}_{0,1}(\tilde{\tau}_{0,1}) = \frac{[Y]_0}{|\alpha_{0,1}|\tilde{\tau}_{0,1}} P(\delta[Y]). \quad (2)$$

Since a time period τ in which $[Y]$ is nearly constant contains roughly $\tau/(\tilde{\tau}_0 + \tilde{\tau}_1)$ CCW (and CW) intervals, the CCW duration-time distribution, $Q_0(\tau_0)$ is simply

$$Q_0(\tau_0) \sim \int_0^\infty d\tilde{\tau}_0 \frac{\tau}{\tilde{\tau}_0 + \tilde{\tau}_1} \tilde{Q}_0(\tilde{\tau}_0) P(\tau_0, \tilde{\tau}_0), \quad (3)$$

with a similar expression for the CW distribution $Q_1(\tau_1)$. If $P(\delta[Y])$ is constant over some range of $\delta[Y]$, say, $\delta[Y]_1 < \delta[Y] < \delta[Y]_2$, then $\tilde{Q}_0(\tilde{\tau}_0) \sim \tilde{\tau}_0^{-1}$ for $\tilde{\tau}_0$ in the range $\tau^{(1)} < \tilde{\tau}_0 < \tau^{(2)}$, where $\tau^{(1,2)} = t_0 \exp(\alpha_0 \delta[Y]_{1,2}/[Y]_0)$. Equation (3) then implies that, for $\tau^{(1)} \gg \tilde{\tau}_1$, the CCW duration-time distribution $Q_0(\tau_0)$ behaves as a power law, $Q_0(\tau_0) \sim \tau_0^{-2}$, in agreement with the recent experimental results [4]. The range of the power-law distribution is $R_0 \equiv \tau^{(2)}/\tau^{(1)} = \exp(\frac{\alpha_0(\delta[Y]_2 - \delta[Y]_1)}{[Y]_0})$. While there is no *a priori* reason to believe that $\delta[Y]$ has a flat distribution, it is reasonable to assume that it follows a Gaussian distribution: $P(\delta[Y]) \sim \exp(-\frac{\delta[Y]^2}{2\Delta[Y]^2})$, with variance $\Delta[Y]^2$. Within the window $-\frac{\Delta[Y]}{2} < \delta[Y] < \frac{\Delta[Y]}{2}$, $P(\delta[Y])$ changes by less than 10% and so is close to constant, whereupon the τ_0 distribution exhibits power-law behavior, τ_0^{-2}, over a range $R_0 \sim \exp(\alpha_0 \frac{\Delta[Y]}{[Y]_0})$.

To test these results, we simulated a model wherein the dynamics of the CheY-P concentration satisfies

$$\frac{d[Y]}{dt} = -\frac{[Y] - [Y]_0}{\tau} + \eta(t), \quad (4)$$

where the first term represents the slow relaxation (adap-

tation) towards a preferred concentration $[Y]_0$ with a long time scale τ, and $\eta(t)$, with $\langle\eta(t_1)\eta(t_2)\rangle = \Delta_0\delta(t_1 - t_2)$, is a Gaussian white noise, representing the fast stochastic driving force. In the simulation, the correlation time for η is taken to be the discrete time unit $\Delta t = 1$. The fluctuation $\delta[Y] \equiv [Y] - [Y]_0$ described by (4) has a stationary Gaussian distribution with variance $\Delta[Y]^2 = \frac{1}{2}\Delta_0\tau$, and the correlation function $\langle\delta[Y](t)\delta[Y](0)\rangle$ decays exponentially with correlation time τ.

To simulate the motor switching behavior, the value of $[Y](t)$ is determined through integration of the stochastic Eq. (4). The corresponding energy barrier for switching is then calculated from the linear model [Eq. (1)], the decision to switch the sense of rotation of the motor being made on the basis of the corresponding switching probability. Figure 2 shows the resulting distribution of CCW duration times for different values of the effective noise strength $\Delta_n \equiv \alpha_0\Delta[Y]/[Y]_0$ and with $\frac{\alpha_1}{\alpha_0} = -\frac{1}{5}$. As our analysis predicts, the CCW duration-time distribution is Poisson-like for zero noise and behaves roughly as $1/\tau_0^2$ for sufficiently large noise. The CW duration distribution (not shown here) remains approximately exponential due to the smallness of its amplification factor α_1.

Power spectra and correlations.—The switching of the bacterial motor can be described by a binary variable $S(t)$, where $S(t) = 1$ for CCW and 0 for CW. The switching statistics can be characterized by the correlation function, $C_s(t) \equiv \langle(S(t + t') - \langle S\rangle)(S(t') - \langle S\rangle)\rangle$, of $S(t)$, or, equivalently, as in [4], the power spectrum $\mathcal{P}(f)$. Here $\langle S\rangle$ is the average value of $S(t)$, i.e., the CW bias. In the simplest approximation, where $C_s(t)$ is assumed dominated by values of t' and $t + t'$ that fall within a single CCW (or CW) interval (the "single-interval approximation"), $C_s(t)$ is
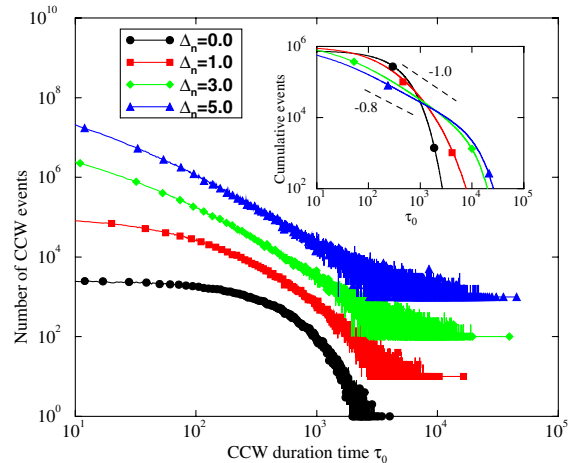

FIG. 2 (color online).   Distribution of CCW duration times for different values of the effective noise strength of the two-state model: $\Delta_n \equiv \alpha_0\Delta[Y]/[Y]_0 = 0.0$, 1.0, 3.0, 5.0, and for $\tau = 6000$, $t_0 = 300$, $t_1 = 30$, and $\alpha_1 = -\alpha_0/5$. Curves are averages over 100 runs, each with run time of 600 000. Curves have been shifted in the y direction for clarity. Inset shows cumulative CCW duration-time distributions.

determined by the distribution function $Q_0(\tau_0)$ alone:
$C_s(t) \sim \int_t^\infty (\tau_0 - t)Q_0(\tau_0)d\tau_0$. If, within a range $\tau^{(1)} < \tau_0 < \tau^{(2)}$, $Q_0(\tau_0)$ is algebraic with exponent $-\beta$ for $\beta > 2$, i.e., $Q_0(\tau_0) \sim \tau_0^{-\beta}$, then $C_s(t) \sim t^{2-\beta}$ in roughly the same range, i.e., $\tau^{(1)} < t < \tau^{(2)}$. For $\beta = 2$, $C_s(t) \sim$ const $- \log(t)$ over that range. $\mathcal{P}(f)$, the Fourier transform of $C_s(t)$, also follows a power law, $\mathcal{P}(f) = \int C_s(t) \times \exp(-2\pi i f t)dt \sim f^{-\gamma}$, within the corresponding frequency range $(2\pi\tau^{(2)})^{-1} < f < (2\pi\tau^{(1)})^{-1}$, the exponents γ and β related by $\gamma + \beta = 3$. For sufficiently large values of $\alpha_0\Delta[Y]/[Y]_0$, $Q_0(\tau_0)$ can fall off as $1/\tau_0^2$ over a sizable time range. In this case, the single-interval approximation predicts that $\mathcal{P}(f) \sim f^{-\gamma}$ with $\gamma = 1$, in rough agreement with the experimental results of Ref. [4], where $\beta \sim 2.2$ and $\gamma \sim 0.8$ for a WT cell, over a range of t or f of around 1.5 decades. As we shall see, however, this agreement may be fortuitous.

To test the single-interval approximation, we calculated $\mathcal{P}(f)$ by solving our model numerically, for different values of the effective noise strength $\Delta_n \equiv \alpha_0\Delta[Y]/[Y]_0$. As shown in Fig. 3(a), all spectra (each one an average over 100 runs of run time 100τ) have the generic $1/f^2$ behavior at high f. For $\Delta_n = 0$, the spectrum becomes constant at lower f, implying the expected exponential decay of $C_s(t)$. For larger Δ_n, the spectra flatten as f decreases before exhibiting apparent power-law behavior at still smaller f,
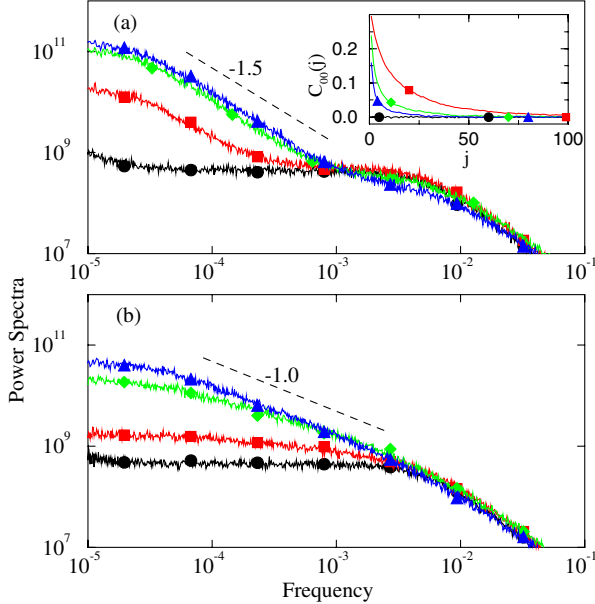

FIG. 3 (color online). Average power spectra for the same parameters as in Fig. 2, and effective noise strengths $\alpha_0\Delta[Y]/[Y]_0$ of 0.0 (circle), 1.0 (square), 3.0 (diamond), and 5.0 (triangle). (a) Data from numerical solution of our model. Inset: CCW/CCW duration-time correlation function $C_{00}(j)$ vs j, for the same set of noise levels. Correlations are absent for the zero-noise curve, but extend out to separations of at least $20-30$ intervals when noise is present. (b) Power spectra for shuffled version of data used in panel (a), as discussed in text.

in qualitative agreement with experimental results from Ref. [4]. At the lowest f's, $f < (2\pi\tau)^{-1}$, the power spectra begin to level off, consistent with $C_s(t) \sim e^{-t/\tau}$ expected for $t \gtrsim \tau$ [or, equivalently, the Lorentzian spectrum $\mathcal{P}(f) \sim \tau/[1 + (2\pi\tau f)^2]$].

The exponent, $\gamma \sim 1.5$, of the apparent power-law regions for the two highest noise levels in Fig. 3(a) exceeds the 1.0 predicted by the single-interval approximation. This is because the approximation misses important correlations between the lengths of nearby CCW (CW) intervals. In the model, such correlations result from the CheY-P level, i.e., $\delta[Y]$, changing little over times less than τ, which far exceeds the typical CCW or CW duration times, τ_0 or τ_1. Thus all the duration times for intervals lying within time τ are strongly correlated, as shown by the correlation functions $C_{00}(j)$, $C_{11}(j)$, and $C_{10}(j)$ between the duration times of pairs of intervals separated by j switches, with respective interval types CCW/CCW, CW/CW, and CCW/CW. For example, $C_{00}(j) \equiv \sigma_0^{-2}\langle(\tau_0(i) - \langle\tau_0\rangle)(\tau_0(i+j) - \langle\tau_0\rangle)\rangle_i$, where $\tau_0(i)$ is the duration time of the ith CCW interval, $\langle\tau_0\rangle$ and σ_0^2 are the mean and variance of the CCW duration-time distribution. The numerical solution of our model shows that these correlations can persist to large values of j. The inset of Fig. 3(a) illustrates this point with plots of the CCW/CCW correlation function $C_{00}(j)$ vs j.

To show the effect of these correlations on $\mathcal{P}(f)$, we took a signal $S(t)$ resulting from the numerical solution of our model, randomly permuted the order in which the CCW intervals appeared, and then randomly permuted the CW intervals, thereby creating a different signal $S'(t)$ with the same distribution of duration times but no duration-time correlations. Figure 3(b) shows the result of averaging $\mathcal{P}(f)$ for 100 different such permutations. The averaged spectra show $1/f$ scaling in the range of f where the single-interval approximation predicts it. Thus the correlations indeed account for the discrepancy between the numerical data and the single-interval approximation.

To verify in the experimental data the existence of these duration-time correlations that are an important prediction of our theory, we also computed $C_{00}(j)$, $C_{11}(j)$, and $C_{10}(j)$ for the longest experimental data set in Ref. [4]. The results, displayed in Fig. 4(a), confirm that duration-time correlations indeed exist in the experimental data, though the curves are noisier than in Fig. 3 because the amount of data is limited. Note the negative correlation between nearby CW and CCW intervals demonstrated by Fig. 4(a). This is consistent with the experiments of Scharf *et al.* [8], who reported opposite dependences of CW and CCW switching rates on changes in CheY-P level. These experiments motivated the choice of different signs for α_0 and α_1 in our model.

The effect of duration-time correlations on the power spectrum can again be demonstrated by randomly permuting the positions of both the CCW and CW intervals in the experimental data set, and then calculating the power
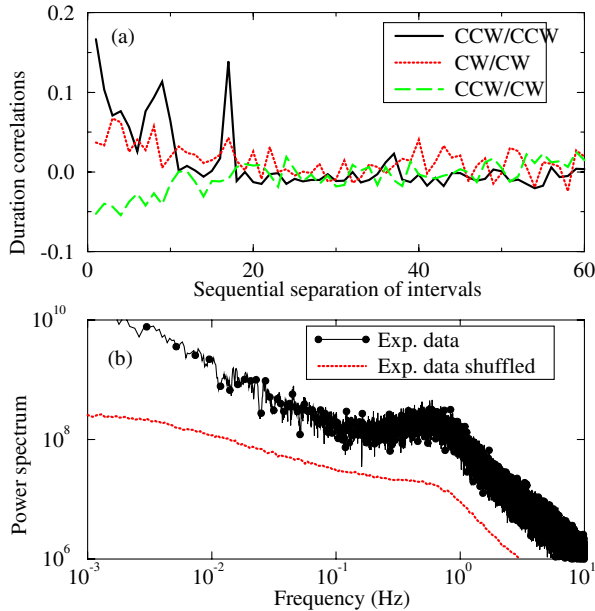
FIG. 4 (color online).   (a) Duration-time correlations C_{00}, C_{11}, and C_{10}, calculated from the experimental data of [4]. C_{00} and C_{11} tend to be positive, and C_{10} tends to be negative. Range of correlation is about 15. (b) Power spectra for original (circle) and shuffled (solid line, shifted in the y direction for clarity) experimental data differ significantly in the low frequency range.

spectrum for the shuffled data. The result, averaged over 100 shuffled data sets, is shown in Fig. 4(b), together with the original experimental power spectrum. The shuffled data show apparent power-law behavior for frequencies between roughly 0.01 and 1 Hz, with an exponent of about 0.55, while the peak in the experimental data just below 1 Hz is eliminated by the shuffling.

Although we have confirmed the existence of duration-time correlations and their relevance to $\mathcal{P}(f)$ both in the experimental data and in our model, the behavior for intermediate values of f where $\mathcal{P}(f)$ appears to behave as $1/f^{\gamma}$ remains unclear: Our simulations and Ref. [4] find different values of γ, and $\gamma < 1$ in the shuffled experimental data. There may be no true universal behavior in this intermediate frequency range, and the apparent algebraic behavior may simply reflect a nonuniversal crossover between the $1/f^2$ behavior at large f and the Lorentzian behavior at asymptotically small f.

Discussion.—We have seen how power-law distributions of CCW (or CW) interval lengths can arise naturally from the addition to the familiar two-state model of time varying energy barriers caused by fluctuations in the CheY-P concentration $[Y](t)$. For WT *E. Coli* cells, the slow methylation process can result in correlation times τ of the order of minutes for fluctuations in $[Y](t)$, while typical switching times, say, τ_0, are of the order of seconds. Given $\tau \gg \tau_{0(1)}$ [so CheY-P fluctuations do not average out within individual CCW (CW) intervals], we showed that the range R_0 of the power-law CCW distribution

depends on both the relative CheY-P fluctuation and the motor amplification factor: $R_0 \sim \exp(\alpha_0 \Delta[Y]/[Y]_0)$. Since $\frac{\Delta[Y]}{[Y]_0}$ is probably small (<1), large $\alpha_{0(1)}$ is essential for the CCW (CW) power-law distribution to be experimentally observable. Interestingly, recent single-cell experiments show that the motor response to CheY-P concentration changes is ultrasensitive, which implies the amplification factor α_0 is large: as high as 10.3 [9]. Assuming $\alpha_0 \sim 10$, the range of the CCW power-law distribution can then exceed one decade if $\Delta[Y]/[Y]_0 > 0.2$, a reasonable requirement for the relative CheY-P concentration fluctuation. Discussions of the experimental ramifications of our model will be presented elsewhere.

Our model resembles the two-state models believed to explain $1/f$ noise in many physical systems [10]. However, the bacterial motor model is described by a single two-state system with *temporal* variations in the energy barrier, driven by fluctuations in CheY-P concentration. In contrast, the classic model for $1/f$ noise consists of a large ensemble of two-state systems, each having an energy barrier with a fixed but random value, making the variation in energy barrier *spatial*. In the absence of extra correlation among the duration times in the bacterial motor model, both models exhibit $1/f$ noise in their power spectra, $\mathcal{P}(f)$. However, the extra temporal correlations in the motor switching pattern make the behavior of $\mathcal{P}(f)$ more complicated than simple $1/f$; indeed, $\mathcal{P}(f)$ may not exhibit universal power-law behavior.

The relatively small number of molecules involved in biochemical reactions inside cells makes noise in biological systems ubiquitous. In this Letter, we showed how simple, Gaussian concentration fluctuations and the intrinsic nonlinear properties of the underlying biological pathway can produce algebraic run-time distributions and other fascinating temporal behavior of bacterial cells.

[1] H. C. Berg, Phys. Today **53**, No. 1, 24 (2000).
[2] H. C. Berg, Annu. Rev. Biochem. **72**, 19 (2003).
[3] J. J. Falke and G. Hazelbauer, Trends Biochem. Sci. **26**, 257 (2001).
[4] E. Korobkova *et al.*, Nature (London) **428**, 574 (2004).
[5] S. M. Block, J. E. Segall, and H. C. Berg, J. Bacteriol. **154**, 312 (1983).
[6] K. A. Fahrner, Ph.D. thesis, Harvard University, 1995.
[7] S. Khan and R. M. Macnab, J. Mol. Biol. **138**, 563 (1980).
[8] B. E. Scharf, K. A. Fahrner, L. Turner, and H. C. Berg, Proc. Natl. Acad. Sci. U.S.A. **95**, 201 (1998).
[9] P. Cluzel, M. Surette, and S. Leibler, Science **287**, 1652 (2000).
[10] P. Dutta and P. M. Horn, Rev. Mod. Phys. **53**, 497 (1981).